A Simple Model of Stratospheric Dynamics Including Solar Variability

ALEXANDER RUZMAIKIN

Jet Propulsion Laboratory, California Institute of Technology, Pasadena, California

JOHN LAWRENCE AND CRISTINA CADAVID

Department of Physics and Astronomy, California State University Northridge, Northridge, California

(Manuscript received 29 April 2002, in final form 9 September 2002)

ABSTRACT

A simple dynamic model, truncated from the stratospheric wave–zonal flow interaction Holton and Mass model, is introduced and studied. This model consists of three ordinary differential equations controlled by two parameters: the initial amplitude of planetary waves and the vertical gradient of the zonal wind. The changes associated with seasonal variations and with the solar variability are introduced as periodic modulations of the zonal wind gradient. The major climatic response to these changes is seen through modulation of the number of cold and warm winters.

1. Introduction

Variability of the stratosphere, in particular the change in ozone due to the solar UV variations, has been proposed as an important cause of climate change (cf. Haigh 1994; Hartmann et al. 2000; Lean and Rind 2001). The major changes take place in the upper stratosphere (Hood et al. 1993) where variations in the UV radiation are larger by almost two orders of magnitude compared to 0.1% solar cycle variations in the total irradiance (Lean 1987).

Stratospheric dynamics is mainly determined by an interaction between waves, which propagate up in the wintertime from the troposphere, and zonal winds in the stratosphere (Charney and Drazin 1961; Andrews et al. 1987). The waves, constrained by conservation of quasigeostrophic potential vorticity, affect the mean zonal flow through their flux divergence. In midlatitudes these waves are planetary (Rossby) waves generated by thermal and topographic forcing. The importance of this interaction as a possible mechanism that can be influenced by solar variability was indicated in early studies (Bates 1981, and references therein). Current general circulation models [GCMs; see, e.g., Balachandran et al. (1999)] include this interaction but have short time runs (compared to the 11-yr solar cycle) due to high computational cost.

An approximate approach to the dynamics with fine vertical resolution was originated by Holton and Mass (1976, hereafter HM76; see also Holton and Dunkerton 1978) and developed by Yoden (1987, 1990, hereafter Y87 and Y90). These authors confined the integration volume to a latitudinal cut around 60° and, by retaining only one longitudinal and one latitudinal mode, and using finite differences in the vertical, reduced the dynamics to a one-dimensional system of ordinary differential equations with time as the independent variable. Although this one-dimensional model cannot be expected to describe the dynamics realistically, it led to discovery of the stratospheric vacillations. Three major flow regimes predicted by this model were identified in the analysis of satellite data at the top of the stratosphere (Pierce and Fairlie 1993). The general circulation modeling of the stratospheric vacillations also supports the basic finding of the one-dimensional model (Christiansen 1999).

In this paper we use another advantage of the one-dimensional modeling: its capability to handle at a very low computational cost the long-term dynamics, such as that induced in the stratosphere by solar variability. To focus on the long-time behavior we further simplify the model by considering only one vertical level and thus reducing the system to three ordinary differential equations. The reduced system captures the fundamental mechanism of the interaction between the waves and zonal wind and, as we will show, some major properties of the Holton–Mass dynamic system. It allows us to study transitions between different atmospheric states, in particular slow (lasting for many years) transitions that are in practice difficult or impossible to model with

Corresponding author address: Dr. Alexander Ruzmaikin, JPL, California Institute of Technology, 4800 Oak Grove Dr., Pasadena, CA 91109.
E-mail: aruzmaik@pop.jpl.nasa.gov

GCMs. Thus, the long-term statistics of the occurrence of ''warm'' and ''cold'' winters can be revealed. The frequencies of these occurrences might be sensitive to small changes in external forcing and are thus subject to modulation.

2. The dynamic model

Let us briefly describe the construction of our model. We present the mean zonal wind $\overline{u}$ and the geostrophic streamfunction $\Phi' = f_0\psi'$ in the form suggested by HM76, Y87, and Y90:

$$\overline{u}(y, z, t) = U(z, t)\ \sin ly,$$
$$\psi'(x, y, z, t) = \mathrm{Re}[\Psi(z, t)e^{ikx}]e^{z/2H}\ \sin ly,$$

where x, y with corresponding wavenumbers k, l are standard azimuthal and latitudinal coordinates, f_0 is the Coriolis parameter at a given latitude, and H is a mean scale height. The variables U, Ψ (Ψ is complex) are governed by the quasigeostrophic potential vorticity and the zonal wind equations, symbolically

$$\frac{\partial U}{\partial t} = F(\Psi, U, h, \Lambda), \tag{1}$$

$$\frac{\partial \Psi}{\partial t} = G(\Psi, U, h, \Lambda). \tag{2}$$

Two control parameters were used by HM76 and Y87: the wave amplitude $h(t) = \Psi(0, t)f_0/g$ at the bottom boundary (g is the gravitational acceleration), and the gradient $\Lambda(t) = dU_R/dz$ of the mean radiative zonal wind assumed to be $U_R(z, t) = U_R(0, t) + \Lambda(t)z$. We use below these two control parameters and fixed the other parameters at their typical atmospheric values. The ''free'' parameter h characterizes the initial amplitudes of planetary waves driving the dynamics. The waves are caused by topography and sea–land contrasts with poor predictable amplitude ranging from zero to several hundred meters. The variance in the parameter Λ is a convenient way to characterize the forcing of the system by the annual (radiative) cycle and solar variability cycle. We assume that the other atmospheric parameters are more robust (less critically influence the dynamics under consideration) compared to the control parameters. In any case, many of them, such as g, or the size of the earth, or the mean scale height, or the thickness of the stratosphere, are well fixed.

The explicit form of Eqs. (1), (2) can be derived from the linearized quasigeostrophic potential vorticity equation and a prediction equation for the mean zonal wind (HM76):

$$\left(\frac{\partial}{\partial t} + \overline{u}\frac{\partial}{\partial x}\right)q' + \beta'\frac{\partial \psi'}{\partial x} + \frac{f_0^2}{\rho}\frac{\partial}{\partial z}\left(\frac{\alpha\rho}{N^2}\frac{\partial \psi'}{\partial z}\right) = 0, \tag{3}$$

$$\frac{\partial}{\partial t}\left[\frac{\partial^2 \overline{u}}{\partial y^2} + \frac{f_0^2}{N^2}\frac{1}{\rho}\frac{\partial}{\partial z}\left(\rho\frac{\partial \overline{u}}{\partial z}\right)\right] = -\frac{f_0^2}{N^2}\frac{1}{\rho}\frac{\partial}{\partial z}\left[\alpha\rho\frac{\partial(\overline{u} - u_R)}{\partial z}\right] + \frac{f_0^2}{N^2}\frac{\partial^2}{\partial y^2}\left[\frac{1}{\rho}\frac{\partial}{\partial z}\left(\rho\overline{v'\frac{\partial \psi'}{\partial z}}\right)\right], \tag{4}$$

where $v' = \partial\psi'/\partial x$, the overbar means averaging over x, and

$$q' = \nabla^2\psi' + \frac{f_0^2}{\rho}\frac{\partial}{\partial z}\left(\frac{\rho}{N^2}\frac{\partial \psi'}{\partial z}\right),$$

$$\beta' = \beta - \frac{\partial^2 \overline{u}}{\partial y^2} - \frac{f_0^2}{\rho}\frac{\partial}{\partial z}\left(\frac{\rho}{N^2}\frac{\partial \overline{u}}{\partial z}\right).$$

Here β is the meridional derivative of the Coriolis parameter, $N^2(=4 \times 10^{-4}\ \mathrm{s}^{-2})$ is the buoyancy parameter, $\rho = \rho_0 \times \exp(-z/H)$ is the density, H (=7 km) is the scale height, and $\alpha = 1.5 + \tanh[(z - 25)/7] \times 10^{-6}\ \mathrm{s}^{-1}$ is the Newtonian cooling/heating rate.

Following HM76, Y87, and Y90, we confine the volume of integration to the latitudinal channel centered at 60°N with meridional extent of 60° latitude and vertical extent z_T (assumed here = 50 km, i.e., at the height where the strongest changes in the solar UV flux are measured). The parameters f_0 and β at this latitude are $1.26 \times 10^{-4}\ \mathrm{s}^{-1}$, and $1.14 \times 10^{-11}\ \mathrm{s}^{-1}\ \mathrm{m}^{-1}$, correspondingly.

The zero normal flow conditions across the side boundary $y = 0, L$ require that ψ' and meridional speed v' vanish at these boundaries. Also $\overline{u} = 0$ there, if it is zero initially. The requirement that the energy density of wave perturbations vanishes at the upper boundary leads to $\rho^{1/2}\psi'(t, z_T) = 0$ (HM76). This translates into the boundary condition $\Psi(z_T, t) = 0$. The second condition at the upper boundary is $\partial U/\partial z|_{z_T} = \partial U_R/\partial z|_{z_T} = \Lambda$ (see Y87; HM76 discussed different choices but note that results are not very sensitive to this boundary condition). For the lower boundary conditions at $z = 0$ we choose the simple conditions employed in Y90, which specify a wave disturbance and sustain winter westerlies at the ground:

$$\Psi(0, t) = \frac{g}{f_0}h(t), \qquad U(0, t) = U_R(0).$$

For the runs described below the bottom speed is taken to be $U_R(0) = 10\ \mathrm{m\ s}^{-1}$.

The choice of location for the lower boundary $z = 0$ does not affect our calculations below but may impact the interpretation of the results. Note that HM76 put this boundary at the top of the troposphere, Y87 put it at sea level. The actual dynamics of the wave–flow interaction in the troposphere relates the zonal wind and wave perturbations so that on timescales exceeding days they cannot be considered independent. The ground perturbation $\Psi(0, t)$ could be a sensitive function of the

stratospheric wind in a certain range of U (Bates 1981). Our main purpose here is to study the role of a weak solar forcing that acts in the upper stratosphere and to identify the basic nonoscillating stationary states and transitions between them; we do not treat the dynamics near the lower boundary realistically and employ the above simplest lower boundary conditions. We will use also the constant wave perturbation h at $z = 0$ when considering the long (seasonal and decadal) timescales. The constant h in this case can be treated as a statistical winter mean source independent of the low-frequency dynamics in the stratosphere. A recent observational study by Hu and Tung (2002) shows that the Eliasson–Palm (EP) flux of the planetary waves did not show a trend or decadal variations at least within the last 30 years. Because the major causes of waves are near sea level (topography and sea–land contrasts) or perturbations in the troposphere, which are not driven by solar variability, this approach looks reasonable for our goal of studying the solar variability influence on climate. This also allows us to keep only three dynamical equations and avoid short timescale complications.

The selected lower boundary conditions do not include a back action of the dynamics on the boundary. Lower boundary conditions, for which the ground wave and zonal wind perturbations are dynamically related to each other, were introduced by Wakata and Uryu (1987) from kinematic considerations of the flow over a given topography. Our model can be extended to include these boundary conditions. However, it will increase the number of dynamic equations to five; such a system requires a separate study.

With the use of the single-l-mode presentation and the approximation $\sin^2 ly \approx (8/3\pi)\sin ly$, valid in the latitudinal channel under consideration, Eqs. (3), (4) are reduced to the equations for the amplitudes $\Psi(z, t)$ and $U(z, t)$ first obtained by HM76 [see Eqs. (9),(10) in HM76, or Eqs. (2.3)–(2.4) in Y87]. In this reduction, the critical nonlinear term $v'\partial\psi'/\partial z$ that couples the mean zonal wind equation with the equation for the waves transforms into the term proportional to $\mathrm{Im}(\Psi\partial^2\Psi^*/\partial z^2)$.

By setting up finite differencing

$$\left.\frac{\partial\Psi}{\partial z}\right|_{z=j\Delta z} = \frac{\Psi_{j+1} - \Psi_{j-1}}{2\Delta z},$$

$$\left.\frac{\partial^2\Psi}{\partial z^2}\right|_{z=j\Delta z} = \frac{\Psi_{j+1} - 2\Psi_j + \Psi_{j-1}}{(\Delta z)^2}, \quad j = 0, 1, \ldots, 28,$$

with similar expressions for the derivatives of U, Yoden reduced Eqs. (3), (4) to 81 ordinary differential equations that were studied for $l = 3/a = 4.71 \times 10^{-7}\ \mathrm{m}^{-1}$, $k = 2/(a\cos 60^\circ) = 6.28 \times 10^{-7}\ \mathrm{m}^{-1}$, where a is the earth's radius. Dynamical properties of those equations were also investigated by Chao (1985) and Christiansen (2000).

Here we make a more dramatic simplification and consider the simplest case $j = 0, 1, 2$, thus reducing the system to just three ordinary differential equations for the variables defined at the middle height $z_T/2$, with $\Delta z = z_T/2$ and the boundary conditions taken into account at the top and bottom. Thus,

$$\frac{\partial\Psi}{\partial z} = \frac{\Psi_2 - \Psi_0}{2\Delta z} = -\frac{gh}{f_0 z_T},$$

$$\frac{\partial^2\Psi}{\partial z^2} = \frac{\Psi_2 - 2\Psi_1 + \Psi_0}{(\Delta z)^2} = -\frac{8\Psi}{z_T^2} + \frac{4gh}{f_0 z_T^2},$$

$$\frac{\partial U}{\partial z} = \frac{U_2 - U_0}{2\Delta z} = \frac{U_1 - U_R(0) + \Lambda z_T/2}{z_T},$$

$$\frac{\partial^2 U}{\partial z^2} = \frac{U_2 - 2U_1 + U_0}{(\Delta z)^2} = -\frac{4(U_1 - U_R(0) - \Lambda z_T/2)}{z_T^2}.$$

By doing this we obviously lose the vertical dependence but, as we show, still retain the main dynamic properties of the system. The wave streamfunction is then presented in the form $\Psi = X(t) + iY(t)$, so that $(X^2 + Y^2)^{1/2}$, and arctan (Y/X) are the amplitude and phase of the waves. To simplify the notation, we now denote $U_1(t) \equiv U(t)$.

A lengthy but straightforward reduction of the equation for Ψ and U yields[1]

$$\dot{X} = -X/\tau_1 - rY + sUY - \xi\Psi_0 + \delta_w\dot{\Psi}_0, \quad (5)$$

$$\dot{Y} = -Y/\tau_1 + rX - sUX + \zeta\Psi_0 U, \quad (6)$$

$$\dot{U} = -(U - U_R)/\tau_2 - \eta\Psi_0 Y - \delta_\Lambda\dot{\Lambda}, \quad (7)$$

where $U_R = U_R(z_T/2) = U_R(0) - \Lambda z_T/2$ and the overdot signifies a time derivative. Note that the parameter Λ can equally be replaced by the parameter U_R. The system has a converging phase volume, that is, $\mathrm{div}(\dot{X}, \dot{Y}, \dot{U}) < 0$, and includes quadratic nonlinear coupling. Note that the control parameters h, Λ can be time dependent; see the last two terms in Eqs. (5) and (7). The expressions for the other parameters of this system through standard atmospheric parameters are given in the appendix. For our runs we use the following dimensionless numerical values: $\tau_1 = 122.63$, $\tau_2 = 30.37$, and $r = 0.65[1 - 0.97U_R(0) + 10^{-3}\Lambda]$ [$\approx$0.62 for $U_R(0) = 10$ m s^{-1} and $\Lambda = 1$ m s^{-1} km^{-1}], $s = 1.97$, $\xi = 1.66 \times 10^{-3}$, $\zeta = 0.23$, $\eta = 86.90$, $\delta_w = 0.07$, $\delta_\lambda = 5 \times 10^{-4}$ calculated (see appendix) with the same numerical values for atmospheric parameters as Y87. For the transformation to the physical units, note that the time T should be multiplied by ''days,'' distance L by the earth radius, and that the wave variables X, Y have the dimension $[L^2/T]$. Having analytical expressions for the parameters (see appendix) is one of the benefits of having such a simple system.

To better understand the physical meaning of the basic parameters we write down the expression for the relaxation times in Eqs. (5)–(7):

[1] For the sake of control these calculations were carried out by us independently; one of us used a Mathematica routine.

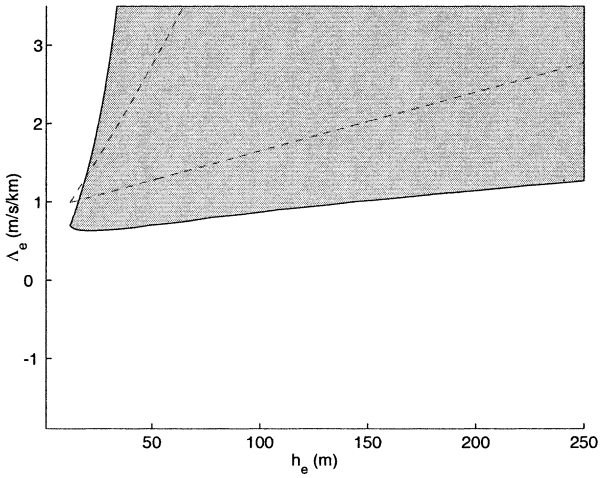

FIG. 1. Equilibrium states of the dynamic system (5)–(7). The shaded area corresponds to the parameter space h_e, Λ_e in which all three equilibrium solutions are real. For comparison, the external boundary of the equivalent region found in Y90 is outlined by the dashed curve.

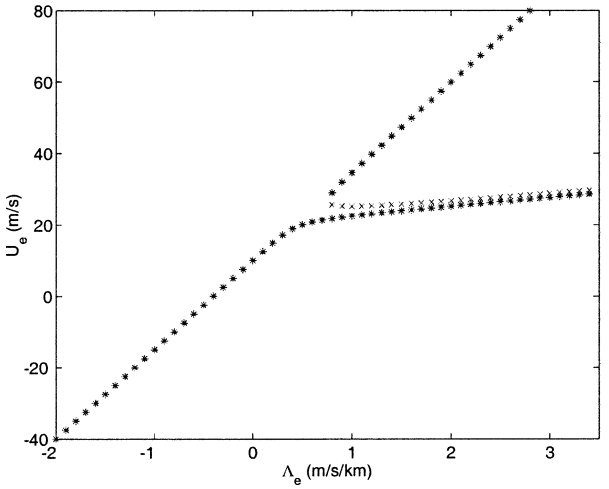

FIG. 2. Three equilibrium states of the zonal wind as functions of the equilibrium gradient of the zonal wind at a fixed initial planetary wave amplitude h_e = 68 m. The unstable solution is marked by crosses. Positive Λ corresponds to winter conditions.

$$\tau_1 = \frac{1}{\alpha}\left[\frac{1 + 32\frac{H^2}{z_T^2} + 4(k^2 + l^2)H^2\frac{N^2}{f_0^2}}{1 + 32\frac{H^2}{z_T^2} - \frac{2H}{\alpha}\frac{\partial\alpha}{\partial z}}\right], \quad (8)$$

$$\tau_2 = \frac{1}{\alpha}\left[\frac{1 + 4\frac{H}{z_T} + l^2Hz_T\frac{N^2}{f_0^2}}{1 + 4\frac{H}{z_T} - \frac{H}{\alpha}\frac{\partial\alpha}{\partial z}}\right]. \quad (9)$$

Thus, the cooling time for the waves and heating/cooling time for the mean zonal wind are different and are not simply $1/\alpha$. The wavenumber k obviously does not enter into τ_2; the ratios z_T/H, f_0/N, as well as the rate of change for α are equally important.

3. Equilibrium states

First we define the equilibrium states of the system (denoted by the subscript e) by zeroing all time dependencies. Then Eqs. (5), (7) can be reduced to a cubic equation for any of the variables. Depending on the parameters h_e, Λ_e this cubic equation has either three real, or one real and two complex conjugated solutions. We are interested in the range of parameters h_e, Λ_e when all three solutions are real (shaded area in Fig. 1). Figure 1 is similar to the diagram based on 81 equations (see Fig. 1 in Y90). This validates in part our truncation. Figure 2 shows an example of the equilibrium solutions as functions of the zonal wind gradient for a fixed h_e = 68 m. Linear stability analysis shows that the highest and lowest solutions are linearly stable. The middle solution is linearly unstable. We found that the separation between the top and the other two solutions increases with increasing h_e. Figure 3 shows how these equilibrium solutions depend on the parameter h_e for a fixed Λ_e.

Transitions from the upper to the lower branch can be induced by seasonal winter–summer variations that switch the sign of the zonal wind gradient. In winter conditions (positive Λ_e) the lower branch corresponds to the presence of stratospheric warmings. In addition to the seasonal variation we also consider here variations simulating the solar cycle. We induce the transitions by periodic variations of the parameter Λ_e; see Eq. (8). If we interpret the two stable states as potential wells and the unstable one as a potential hump in between, these variations can be viewed as changes in the shape of the

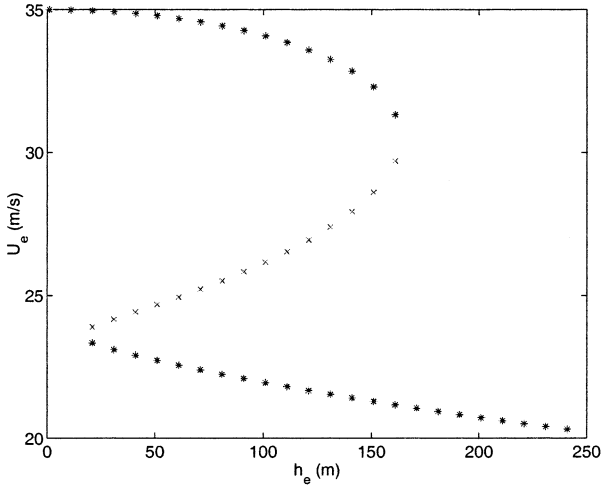

FIG. 3. Three equilibrium states of the zonal wind as function of the initial planetary wave amplitude at a fixed equilibrium gradient of zonal wind Λ_e = 1 m s^{-1} km^{-1}. The unstable solution is marked by crosses. Small h corresponds to large winter amplitudes and large h to small winter amplitudes.

potential somewhat similar to periodic changes of potential used in stochastic resonance theory (Nicolis 1982). During the course of a year, the system passes from the double-well regime in the winter to the single-well regime in the summer. Each autumn the system ''chooses'' which of the double wells to occupy over the following winter. This choice between a cold or warm winter can be extremely sensitive to changes in the system parameters or external perturbations.

4. Annual and solar cycle variations

We introduce seasonal and solar cycles through variations in Λ:

$$\Lambda = \Lambda_0 + \delta\Lambda_a \sin\left(\frac{2\pi t}{1\ \mathrm{yr}}\right) + \delta\Lambda_s \sin^2\left(\frac{\pi t}{11\ \mathrm{yr}}\right). \quad (10)$$

In the numerical run of Eqs. (5)–(7) presented earlier, we follow Y90 and use $\Lambda_0 = 0.75$ m s^{-1} km^{-1} and $\delta\Lambda_a = 2.25$ m s^{-1} km^{-1}. The simplest limit case, with no solar forcing ($\delta\Lambda_s = 0$) and no coupling between the zonal wind and the wave, has been investigated in Y90. In this case, the seasonal forcing cannot cause interannual variability because there is no memory with timescales longer than a year in the low-heat capacity stratosphere; therefore, the time evolution in a winter is cleared in the following summer. However, this (memory) argument is not valid for the system (5)–(7) with coupling of the variables and nonlinearity. The system, depending on parameters, shows a richer response even to seasonal forcing; see below. Solar variability forcing ($\delta\Lambda_s \neq 0$) further changes the situation introducing a new (decadal) variation.

The magnitude of changes induced by solar variability is not certain. Cycle variations of the total solar irradiance reaching the earth's atmosphere are 0.1% over the solar cycle (Hoyt and Schatten 1997). Variations of the solar UV radiation are larger by almost two orders of magnitude, but they do not reach the earth's surface directly, affecting instead the upper stratosphere (Hood et al. 1993; Lean and Rind 2001) and causing temperature and ozone changes there. The effect of these variations, however, can reach the earth through interrelation of stratospheric dynamics with the troposphere circulation (Thompson and Wallace 1998; Baldwin and Dunkerton 1999). We estimate the amplitude of $\delta\Lambda_s$ as follows.

The 11-yr cycle in the solar UV flux influences the ozone and produces temperature changes of about 1–3 K near the equatorial part of the top of the stratosphere (Hood et al. 1993). This induces a latitudinal gradient of temperature and, hence, in accord with the geostrophic thermal wind equation, a vertical gradient in the zonal wind. Thus, we can simulate the changes related to the solar cycle by periodically modulating the parameter Λ. To roughly evaluate the amplitude of these variations we take the variation of the thermal wind equation

$$\frac{\partial U}{\partial z} = -\frac{R}{fH}\frac{\partial T}{\partial y} \quad (11)$$

with the gas constant $R = 2.87 \times 10^6$ cm^2 s^{-2} K^{-1}, scale height $H = 7$ km, and the Coriolis parameter $f = 10^{-4}$ s^{-1}. The meridional extent δy from the equator to 60° is approximately one earth radius. This gives amplitude

$$\delta\Lambda_s \approx 4 \times 10^4 \frac{\delta T}{\delta y} \approx 0.1\ \mathrm{m\ s^{-1}\ km^{-1}} \quad (12)$$

when $\delta T = 2$ K. Thus the amplitude of cycle variations may be as large as 10% of Λ_0($\approx$1 m s^{-1} km^{-1}).

Numerical integration of Eqs. (5)–(7) shows that the system oscillates between positive and negative zonal winds. For small h (roughly $<$ 60 m) the oscillations proceed only with large winter (positive) zonal mean wind. For large h (roughly $>$ 75 m) the winter winds are small. In the middle range of h the system undergoes apparently irregular transitions from large to small winter winds, slipping from one equilibrium solution to the other. These transitions are modulated by solar cycle variations.

Examples of the solutions are shown in Fig. 4 where we set a constant initial wave amplitude $h = 68$ m and gradually increase $\delta\Lambda_s = \epsilon\Lambda_0$ by changing ϵ from 0 to 0.3. With no solar cycle variations (upper panel), strong winter winds alternate with weak winds. At small h, these alternations follow the annual cycle, as indicated by Y90, and can be seen directly from Eq. (7) above. More exactly, when $h = 0$ the phase delay to a periodic forcing in Eq. (7), determined by $2\pi\tau_2/365 \approx 0.5 < 1$, is not large. Hence, a periodic forcing induces a periodic response. At small $h \neq 0$ the system can transit from the low to high branch at the limit points in the equilibrium diagram (see Fig. 2). The increase of h introduces more complicated behavior of U. Thus, in the case shown in Fig. 4 one can see the biennial oscillations, which originate due to a strong coupling of the mean wind to the wave [see Eq. (7)] and the nonlinearity of the system. The oscillations are regular only for this particular value of h; they become irregular when h is changed. Biennial oscillations of potential vorticity in the Northern Hemisphere are, in fact, observed at middle to high latitudes (Baldwin and Dunkerton 1998). Our model therefore indicates a possible mechanism causing these oscillations. To illustrate how the dynamic behavior is related to the equilibrium states we superimpose a model trajectory, for the case $\epsilon = 0$, $h = 68$ m, on the equilibrium diagram in the U, Λ plane (Fig. 5).

When h is very large, one of the limit points is outside the annual range of Λ_a; hence, no transitions are possible and the system selects the lower branch every winter. The solar influence (through the parametric changes in the vertical gradient of zonal wind) results in cycle modulation of the number of weak wind (warm) winters, superimposed on the effects produced by the annual variations.

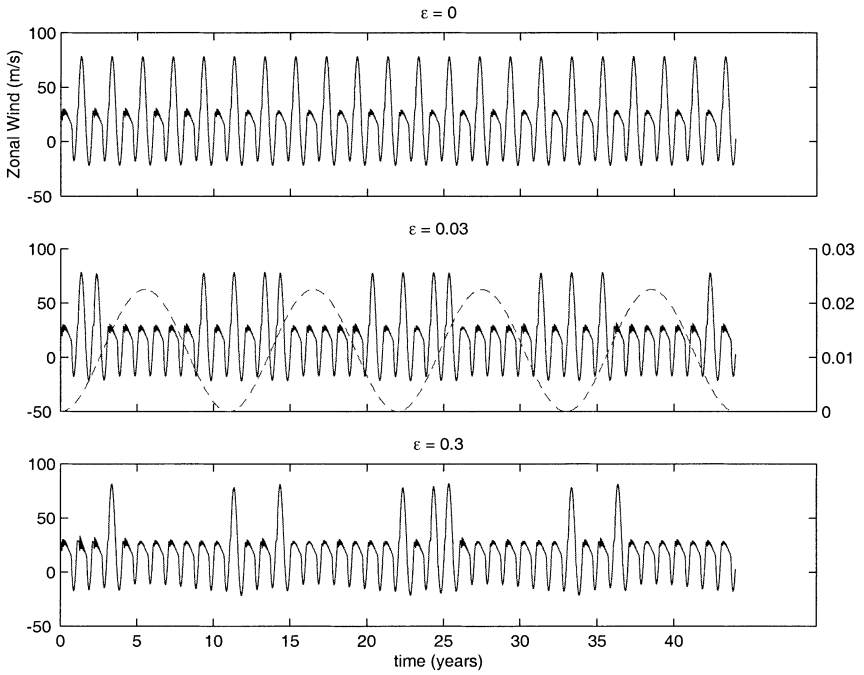

FIG. 4. Zonal wind variations with (upper) annual only and (middle), (lower) both annual and solar cycle periodic changes in Λ. The parameters used for this run are $h = 68$ m, $\Lambda_0 = 0.75$ m s^{-1} km^{-1}, $\Lambda_a = 2.25$ m s^{-1} km^{-1}, and three values of $\Lambda_s = \epsilon\Lambda_0$ with the values of ϵ shown on tops of the panels. The value $\Lambda_s = 0.1$ m s^{-1} km^{-1} discussed in the text fits into the interval 0.03–0.3 m s^{-1} km^{-1}. The rhs axis in the second panel shows the amplitude of the solar forcing.

5. Discussion

Eqs. (5)–(7) define a very simple model of interaction of planetary waves, propagating upward from the earth's surface, with zonal winds in the stratosphere. Although the use of a single meridional wave mode does not allow the consideration of horizontal fluxes, the model maintains some important global features of atmospheric dynamics.

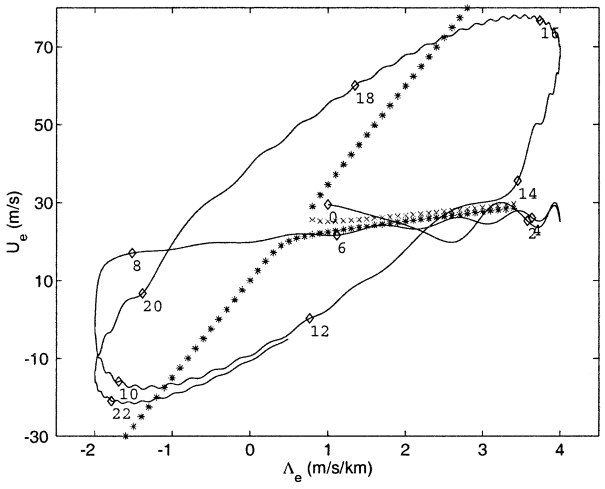

FIG. 5. A time behavior of the mean zonal wind, calculated from Eqs. (5)–(7) driven only by the annual cycle ($\epsilon = 0$), superimposed on the equilibrium diagram in Fig. 2. The initial wave amplitude is $h = 68$ m. The trajectory is plotted for 2 yr. The numbers on the trajectory mark 4-months intervals.

It is not completely clear how the stratospheric changes can affect the troposphere, but it appears that the stratosphere–troposphere interface may involve a leading mode of the atmospheric variability. This mode of wintertime atmospheric variability, called the North Annular Mode (NAM), in the Northern Hemisphere accounts for 22% of the variance in geopotential height at the sea level (Thompson and Wallace 1998) and 23% of the variance in the five-level dataset (1000, 300, 100, 30 and 10 hPa; Baldwin and Dunkerton 1999). It has an almost longitudinally symmetric structure extending from sea level, through the troposphere, to the top of the stratosphere. The mode is sensitive to rather modest external forcing (Thompson and Wallace 1998). There are indications that its interannual variability can be forced by stratospheric perturbations that propagate downward to the troposphere (Baldwin and Dunkerton 1999; Black 2002). In particular, its interannual variability can be forced by solar cycle variations (Ruzmaikin and Feynman 2002). An interesting question is, can equilibrium states found here for the 3-equation system, and earlier by Yoden for the 81-equation system, possibly be identified with the basic states of the NAM mode? The transitions between these states can then be induced by seasonal variations in Λ and modulated by solar cycle changes.

The identification of the equilibrium states with two

basic states of the NAM mode would lead us to a climate interpretation of the results Fig. 3. Because positive NAM index (strong positive winds) means cold winters, we see that, at least for the selected set of parameters, our model predicts more warm winters at solar maxima, as seen in the middle panel in Fig. 4. (The sign of the correlation, however, is sensitive to the choice of Λ_0. As Λ_0 is changed by 10s of percents, one passes through alternating correlation regimes. Likewise, the qualitative behavior of the system is preserved when h is changed by up to ~20%.) This seems to be in qualitative agreement with the study of correlations between the NAM mode and cycle variations (Ruzmaikin and Feynman 2002) and earlier reported correlations between the solar activity and polar temperature in the stratosphere (Labitzke and van Loon 1999; Kodera 1995). All of these authors separated the data for periods of the east and the west phase of the quasi-biennial oscillation (QBO). Our model does not include this separation. In a more extended study we plan to use more realistic low boundary conditions [relating $\Psi(0, t)$ and the zonal wind] and simulate the east–west QBO conditions. Volcanic disturbances could also be modeled through random variations in the parameter Λ. Anthropogenic influence could be simulated by adding a trend to Λ.

Acknowledgments. We thank the referees for the helpful critical comments. This work supported in part by the Jet Propulsion Laboratory of the California Institute of Technology, under a contract with the National Aeronautics and Space Administration.

APPENDIX

Parameters of Eqs. (5)–(7)

Here we give the exact expressions for the parameters of Eqs. (5)–(7). For this purpose it is convenient to present the system in a canonical form,

$$\begin{aligned}
a(1)\dot{X} &= a(2)X + [a(3) + a(4)\Lambda + a(5)U_B]Y \\
&\quad + a(6)YU + a(7)h + a(8)\dot{h}, \\
a(1)\dot{Y} &= a(2)Y - [a(3) + a(4)\Lambda + a(5)Ub]X \\
&\quad - a(6)XU + a(9)hU, \\
b(1)\dot{U} &= b(2)(U - U_B + \Lambda z_T/2) + b(3)hY + b(4)\dot{\Lambda},
\end{aligned}$$

where

$$\begin{aligned}
a(1) &= k^2 + l^2 + \frac{f_0^2}{N^2}\left(\frac{1}{4H^2} + \frac{8}{z_T^2}\right), \\
a(2) &= \frac{f_0^2}{N^2}\left[\frac{1}{2H}\frac{\partial\alpha}{\partial z} - \alpha\left(\frac{1}{4H^2} + \frac{8}{z_T^2}\right)\right], \\
a(3) &= -k\beta, \\
a(4) &= \frac{8k}{3\pi}\frac{f_0^2}{N^2}\left(\frac{2}{z_T} - \frac{1}{2H}\right), \\
a(5) &= \frac{8k}{3\pi}\frac{f_0^2}{N^2}\left(\frac{4}{z_T^2} + \frac{1}{Hz_T}\right), \\
a(6) &= \frac{8k}{3\pi}\left[k^2 + \frac{f_0^2}{N^2}\left(\frac{1}{4H^2} + \frac{4}{z_T^2} - \frac{1}{Hz_T}\right)\right], \\
a(7) &= \frac{f_0^2}{N^2}\frac{g}{z_T f_0}\left(-\frac{\partial\alpha}{\partial z} + \frac{4\alpha}{z_T}\right), \\
a(8) &= \frac{4f_0^2}{z_T^2 N^2}\frac{g}{f_0}, \\
a(9) &= \frac{32k}{3\pi z_T^2}\frac{f_0^2}{N^2}\frac{g}{f_0}, \\
b(1) &= l^2 + \frac{f_0^2}{N^2}\left(\frac{4}{z_T^2} + \frac{1}{Hz_T}\right), \\
b(2) &= \frac{f_0^2}{N^2}\left[\frac{1}{z_T}\frac{\partial\alpha}{\partial z} - \alpha\left(\frac{4}{z_T^2} + \frac{1}{Hz_T}\right)\right], \\
b(3) &= -\frac{16kl^2}{3\pi z_T^2}\frac{f_0^2}{N^2}\frac{g}{f_0}\exp\left(\frac{z_T}{2H}\right), \\
b(4) &= -\frac{f_0^2}{N^2}\left(\frac{1}{2H} - \frac{2}{z_T}\right).
\end{aligned} \tag{A1}$$

The parameters in Eqs. (5)–(7) are related to these coefficients as follows:

$$\begin{aligned}
\tau_1 &= -\frac{a(1)}{a(2)}, \qquad r = -\frac{[a(3) + a(4)\Lambda + a(5)U_B]}{a(1)}, \\
s &= \frac{a(6)}{a(1)}, \qquad \xi = -\frac{a(7)}{a(1)}, \qquad \zeta = -\frac{a(9)}{a(1)}, \\
\delta_w &= \frac{a(8)}{a(1)}, \qquad \tau_2 = -\frac{b(1)}{b(2)}, \qquad \eta = -\frac{b(3)}{b(1)}, \\
\delta_\Lambda &= \frac{b(4)}{b(1)}.
\end{aligned} \tag{A2}$$

REFERENCES

Andrews, D. G., J. R. Holton, and C. B. Leovy, 1987: *Middle Atmosphere Dynamics.* International Geophysical Series, Vol. 40, Academic Press, 489 pp.

Balachandran, N. K., D. Rind, P. Lonergan, and D. T. Shindell, 1999: Effects of solar cycle variability on the lower stratosphere. *J. Geophys. Res.*, **104,** 27 321–27 339.

Baldwin, M. P., and T. J. Dunkerton, 1998: Biennial, quasi-biennial, and decadal oscillations of potential vorticity in the Northern Hemisphere. *J. Geophys. Res.*, **103,** 3919–3928.

——, and ——, 1999: Propagation of the Arctic Oscillation from the stratosphere to the troposphere. *J. Geophys. Res.*, **104,** 30 937–30 946.

Bates, J. R., 1981: A dynamical mechanism through which variations in solar ultraviolet radiation can influence tropospheric climate. *Sol. Phys.*, **74,** 399–415.

Black, R. X., 2002: Stratospheric forcing of surface climate in the Arctic Oscillation. *J. Climate*, **15,** 268–277.

Chao, W. C., 1985: Sudden stratospheric warmings as catastrophes. *J. Atmos. Sci.,* **42,** 1631–1646.

Charney, J. G., and P. G. Drazin, 1961: Propagation of planetary-scale disturbances from the lower into the upper atmosphere. *J. Geophys. Res.,* **66,** 83–109.

Christiansen, B., 1999: Stratospheric vacillations in a general circulation model. *J. Atmos. Sci.,* **56,** 1858–1872.

——, 2000: Chaos, quasiperiodicity, and internal variability: Studies of a stratospheric vacillation model. *J. Atmos. Sci.,* **57,** 3161–3173.

Haigh, J. D., 1994: The role of stratospheric ozone in modeling the solar radiative forcing of climate. *Nature,* **33,** 544–546.

Hartmann, D. L., J. M. Wallace, V. Limpasuvan, D. W. J. Thompson, and J. R. Holton, 2000: Can ozone depletion and global warming interact to produce rapid climate change? *Proc. Natl. Acad. Sci. USA,* **97,** 1412–1417.

Holton, J. R., and C. Mass, 1976: Stratospheric vacillation cycles. *J. Atmos. Sci.,* **33,** 2218–2225.

——, and T. J. Dunkerton, 1978: On the role of wave transience and dissipation in stratospheric mean flow vacillations. *J. Atmos. Sci.,* **35,** 740–744.

Hood, L. L., J. L. Jiricovich, and J. P. McCormack, 1993: Quasi-decadal variability of the stratospheric influence on long-term solar ultraviolet variations. *J. Atmos. Sci.,* **50,** 3949–3958.

Hoyt, D. V., and K. H. Schatten, 1997: *The Sun and Climate Change.* Cambridge University Press, 279 pp.

Hu, Y., and K. K. Tung, 2002: Interannual and decadal variations of planetary wave activity, stratospheric cooling, and Northern Hemisphere annular mode. *J. Climate,* **15,** 1659–1673.

Kodera, K. M., 1995: On the origin and nature of the interannual variability of the winter stratospheric circulation in the Northern Hemisphere. *J. Geophys. Res.,* **100,** 14 077–14 087.

Labitzke, K., and H. van Loon, 1999: *The Stratosphere.* Springer, 179 pp.

Lean, J., 1987: Solar ultraviolet variations: A review. *J. Geophys. Res.,* **92,** 839–868.

——, and D. Rind, 2001: Earth's response to a variable Sun. *Science,* **292,** 234–236.

Nicolis, C., 1982: Stochastic aspects of climatic transitions—Response to periodic forcing. *Tellus,* **34,** 1–9.

Pierce, R. B., and T. D. A. Fairlie, 1993: Observational evidence of preferred flow regimes in the Northern Hemisphere winter stratosphere. *J. Atmos. Sci.,* **50,** 1936–1949.

Ruzmaikin, A., and J. Feynman, 2002: Solar influence on a major mode of atmospheric variability. *J. Geophys. Res.,* **107** (D14), 4209, doi:10.1029/2001JD001239.

Thompson, D. W. J., and J. M. Wallace, 1998: The Arctic Oscillation signature in the wintertime geopotential height and temperature fields. *Geophys. Res. Lett.,* **25,** 1297–1300.

Wakata, Y., and M. Uryu, 1987: Stratospheric multiple equilibria and seasonal variations. *J. Meteor. Soc. Japan,* **65,** 27–42.

Yoden, S., 1987: Bifurcation properties of a stratospheric vacillation model. *J. Atmos. Sci.,* **44,** 1723–1733.

——, 1990: An illustrative model of seasonal and interannual variations of the stratospheric circulation. *J. Atmos. Sci.,* **47,** 1845–1853.